water

MDPI

Article

Changes of Reference Evapotranspiration and Its Relationship to Dry/Wet Conditions Based on the Aridity Index in the Songnen Grassland, Northeast China

Qiyun Ma [1], Jiquan Zhang [1,*], Caiyun Sun [1], Enliang Guo [1], Feng Zhang [1] and Mengmeng Wang [2]

[1] Institute of Natural Disaster Research, School of Environment, Northeast Normal University, Changchun 130024, China; maqy315@nenu.edu.cn (Q.M.); xlsdydnl@126.com (C.S.); guoel675@nenu.edu.cn (E.G.); zhangf093@nenu.edu.cn (F.Z.)

[2] College of Resources and Environment, Northeast Agricultural University, Harbin 150030, China; shinegarden121@163.com

* Correspondence: zhangjq022@nenu.edu.cn; Tel.: +86-135-9608-6467

Academic Editor: Franco Salerno
Received: 22 February 2017; Accepted: 26 April 2017; Published: 29 April 2017

Abstract: Reference evapotranspiration (ET_0) plays an important role in regional dry/wet conditions. Based on the Food and Agriculture Organization of the United (FAO) Penman-Monteith method and daily climate variables, ET_0 was calculated for 21 stations in and around the Songnen Grassland, northeast China, during 1960–2014. The temporal and spatial variations of ET_0 and precipitation (P) were analyzed in the annual, seasonal, and growing season (from April to October) time series using the Mann-Kendall test, Sen's slope estimator, and linear regression coupled with a break trend analysis. A sensitivity analysis was used to detect the key climate parameter contributing to ET_0 change. By linear regression analysis on the relationship between ET_0, P, and the aridity index (AI), the role of ET_0 in determining regional wet/dry conditions was analyzed. Results show a higher ET_0 in the southwest and a lower ET_0 in the northeast, but P was opposite to that of ET_0. Evident decreasing trends of ET_0 in the annual, seasonal, and growing season time series were detected in almost the entire region by the trend analysis methods. For the entire region, the decreasing trend of ET_0 can be linked to the relative humidity and maximum air temperature. The positive contribution of increasing temperature to ET_0 was offset by the effect of the significantly decreasing relative humidity, wind speed, and sunshine duration at the 0.05 level during 1960–2014. In addition, the value of ET_0 was higher in drought years and lower in wet years.

Keywords: reference evapotranspiration; climatic change; drought/wet; Songnen Grassland

1. Introduction

Climate change is an indisputable fact and may accelerate hydrological cycles and redistribute global water resources [1,2]. The change has been identified not only in individual parameters, such as temperature or precipitation, but also in integrated parameters, like reference evapotranspiration (ET_0) [3]. ET_0 is one of the vital components of the hydrological cycle and controls the energy and mass exchange between terrestrial ecosystems and the atmosphere [3,4]. It is influenced by many factors including climate factors (e.g., temperature, solar radiation), crop factors (e.g., crop pattern, cropping system), environmental conditions, and water resource management [5]. Changes in ET_0 affect agricultural production, water resource programming, and irrigation systems. The observation of trends in these climate factors can reveal the possible impacts of climate change or climate natural variability on the hydrological cycle, identify the spatial and temporal variation, and determine the

dominant climatic variables affecting ET_0. These trends can be helpful in determining appropriate measures for mitigating the potential damage from climate change or its natural variability effects [6–8]. However, the relationship between changing ET_0 and the dry/wet tendency is not quite clear, though it is crucial for water resource management.

Studies that investigate changes in climate factors have yielded a mixture of results and conclusions about the trends of ET_0 for specific locations during the last few decades. Contrary to the general expectation that an increase in temperature leads to an increase in evapotranspiration, such as in south and southeast Romanian during 1961–2007 and in the semi-arid and humid regions in Iran during 1966–2005 [3,9], some previous studies conclude that evaporation has diminished in the last few decades. In the upper and middle to lower Yangtze River basin, Wang et al. [10] reported a decreasing trend in ET_0 from 1961–2000 based on daily data from 115 meteorological stations. Over a 116-year period (1983–2008), Irmak et al. [11] found a significant decrease in ET_0 in the Platte river basin, USA. The same declining trends were also found in other regions throughout the world, such as New Zealand (from the 1970s to the early 2000s), India (1971–2002), and parts of China (1960–2010) [12–14]. However, an increasing trend in ET_0 was identified in other regions from the 1960s to early 2000s, such as Iran (1965–2005), Northern Eurasia (1948–2005), and parts of Romania (1961–2007) [3,15,16].

Being a typical farming-pastoral ecotone located in the central part of northeast China, the Songnen Grasslands have experienced high spatial and temporal variability in ET_0 and precipitation. This makes the management of water resources difficult in the region. However, to the best of our knowledge, there has been no comprehensive study of the relationships between changes in ET_0 and dry/wet conditions, and especially, the sensitivity of ET_0 to climatic variables in this region. Water is the lifeline for socioeconomic development in the Songnen Grassland, because agriculture and animal husbandry, which heavily depend on precipitation and irrigation, are the main industries in the area. Therefore, understanding ET_0 trends and their role in regional dry/wet conditions could give a scientific basis for regional water resource management and allocation and for the scientific decision-making of preventing flood and drought disaster.

To address the problem of the unclear ET_0 changes in the Songnen Grassland, this study set the following objectives: (1) to evaluate the spatial distribution of the ET_0 and precipitation at the annual, seasonal, and growing season time scales in the Songnen Grassland over the period from 1960–2014; (2) to investigate the temporal trend of ET_0 by using the Mann-Kendall test, and linear regression coupled with a break trend analysis, and the slopes of trend lines using the Sen's slope estimator; (3) to analyze temporal trends in the climatic parameters needed to calculate ET_0 and the sensitivity and trends of ET_0 related to the climatic parameters using the sensitivity analysis method; and (4) to explore the role of changing ET_0 in regional dry or wet conditions based on the aridity index (AI). The results of this study will improve our understanding of the impact of climate change or climate natural variability on regional hydrological processes and agricultural irrigation management.

2. Materials and Methods

2.1. Study Area

The Songnen Grassland is located in central northeast China. It lies from 43°30′ N to 48°05′ N and from 122°12′ E to 126°20′ E, and covers an area of approximately 22,350 km^2 (Figure 1). Generally, the study area is located in the meadow steppe belt of China and is an important grassland in the Eurasian steppe zone. The region is dominated by a temperate continental monsoon climate, with four distinct seasons: quite dry (drought in nine years out of ten), windy springs; warm, rainy summers; sunny, mild autumns; and long, freezing, and dry winters [17,18]. From 1960 to 2014, the mean annual temperature ranged from 1.9 °C in the southwest to 6.2 °C in the northeast, while the mean annual precipitation amount varied from 350 mm in the southwest to 500 mm in the northeast. Meanwhile, the mean annual amount of evaporation is roughly two or three times the precipitation.

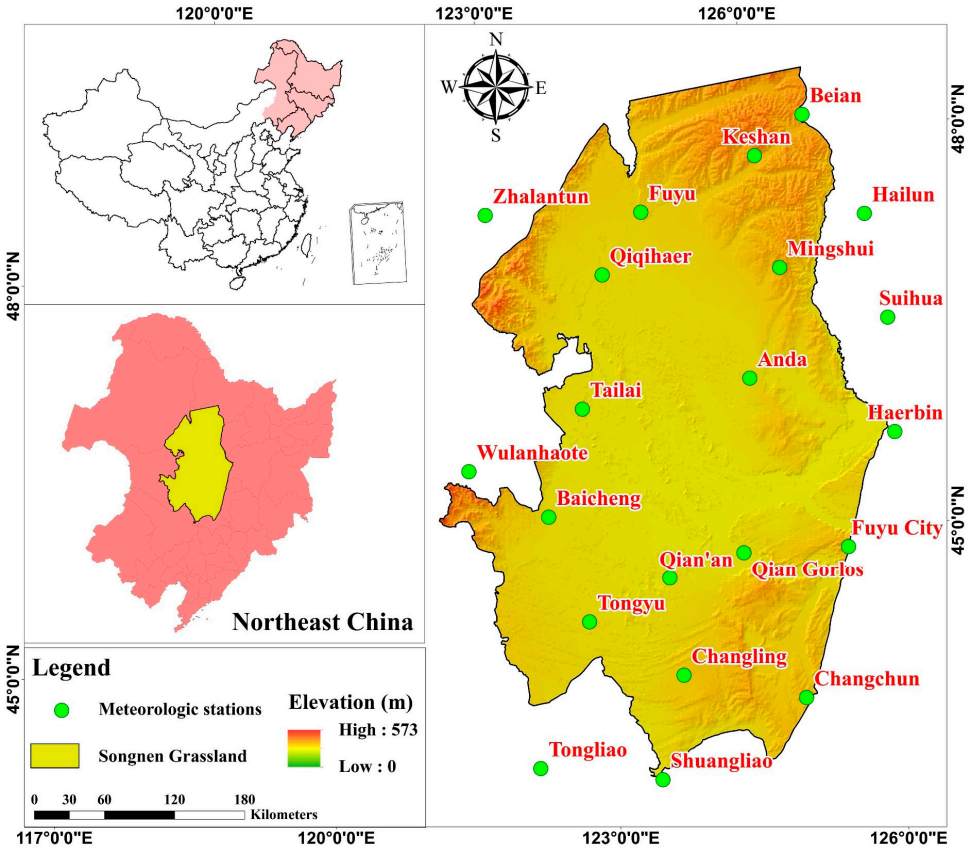

Figure 1. Location of the Songnen Grassland in China and the meteorological stations considered.

The Songnen Grassland forms a typical agricultural area in the east and an agro-pastoral transition zone in the west, determined by various physical geographical features and regional climatic differences [17]. The current ecological environment tends to be deteriorating (e.g., grassland degradation, desertification, and alkalization) due to recent and ongoing climate change and land use change in the region. Since agriculture and animal husbandry development are the main priorities within the general economic strategy of the region, an investigation of changes in ET_0 and its role in regional dry/wet conditions are needed for agriculture managers and stakeholders.

2.2. Climate Data and Quality Control

Climate data from 21 meteorological observatory stations were provided by the National Meteorological Information Centre of China, including daily observations of maximum air temperature (Max T, °C), minimum air temperature (Min T, °C), average air temperature (Ave T, °C), average relative humidity (Ave RH, %), wind speed (Win S, m/s), sunshine duration (Sun H, h), and precipitation (P, mm), for the period from 1960–2014. The regional values for the seasonal, growing season (from April to October), and annual climatic variables were then calculated by the weighted average or sum method. The weight of every station was obtained by the Thiessen polygon method, which assigns the weight in accordance with the areas of each station [19]. Thermal seasons were considered as winter (December, January, and February), spring (March, April, and May), summer (June, July, and August), and autumn (September, October, and November).

The location of the chosen meteorological stations is shown in Figure 1. They are all distributed inside or adjacent to the study area in order to cover the entire region. All selected stations have good-quality data and meet the QA (Quality assurance)/QC (Quality control) requirements, which means that the spatial distribution of the stations had to cover the entire region, the time series had to be long enough to obtain statistically significant results in trend analyses, and the climate data was

quality controlled by the China Meteorological Administration (http://cdc.cma.gov.cn). The missing data were substituted with the corresponding long-term mean value. Although the infilling of missing data may have a slight influence on the trend analysis for each climatic variable and the computation of ET_0, the effect may be negligible since the missing data are infrequent and account for only 0.05–0.1% of the data.

2.3. Methods

2.3.1. Calculation of Reference Evapotranspiration (ET_0)

The FAO-56 Penman-Monteith (FAO-PM) equation was recommended as the sole and global standard method for ET_0 calculation [5,20]. The method has been widely verified for its accuracy and reliability in various climatologic zones around the world [21,22]. Accordingly, the FAO-PM method was used to estimate the daily ET_0 in this study; and, subsequently the seasonal, growing season, and annual ET_0 values were derived from the daily values. The FAO-PM equation is expressed as:

$$ET_0 = \frac{0.408\Delta(R_n - G) + \gamma \frac{900}{(T+273)} U_2 (e_s - e_a)}{\Delta + \gamma(1 + 0.34U_2)} \quad (1)$$

where ET_0 is the reference evapotranspiration (mm/d), Δ is the slope of the saturation vapor pressure curve at a given air temperature (kPa/°C), R_n is the net radiation at the crop surface (MJ/(m^2·d)), G is the soil heat flux density (MJ/(m^2·d)), γ is the psychrometric constant (kPa/°C), T is the mean daily air temperature at 2 m height (°C), U_2 is the wind speed at 2 m height (m/s), e_s is the saturation vapour pressure (kPa), e_a is the actual vapour pressure (kPa), and $(e_s - e_a)$ is the saturation vapour pressure deficit (kPa).

R_n is the difference between the incoming net shortwave radiation (R_{ns}) and the net outgoing longwave (R_{nl}) radiation. R_{ns} is calculated as

$$R_{ns} = (1 - \lambda) R_s \quad (2)$$

where R_s is the incoming solar radiation (MJ/(m^2·d)) and λ (= 0.23) is the albedo of the hypothetical grass reference crop (dimensionless). R_s was estimated based on the sunshine duration record according to the calibration equation by Croitoru et al. [3].

At the same time, R_{nl} is given by

$$R_{nl} = \sigma \left[\frac{T_{\max,K}{}^4 + T_{\min,K}{}^4}{2} \right] (0.34 - 0.14\sqrt{e_a}) \left(1.35 \frac{R_s}{R_{so}} - 0.35 \right) \quad (3)$$

where σ is the Stefan-Boltzmann constant (= 4.903 × 10^9 MJ/(K^4·m^2·d)); $T_{\max,K}$ is the maximum absolute temperature during the 24-h period (K = °C + 273.15); $T_{\min,K}$ is the minimum absolute temperature during the 24-h period (K = °C + 273.15); and R_{so} is the clear-sky radiation (MJ/(m^2·d)). All of the variables in Equation (1) were calculated using the standard procedure outlined by Allen et al. [20]. The monthly time series of ET_0 during 1960–2014 were obtained based on the calculation of ET_0 using the CROPWAT 8.0 software developed by FAO (http://www.fao.org/land-water/databases-and-software/cropwat).

2.3.2. Trend Analysis

To calculate trends, six data sets, including one annual, four seasonal, and one growing season, were obtained for each meteorological station. In this study, the Mann-Kendall (MK) test, a non-parametric test recommended by the World Meteorological Organization (WMO), was used to detect trends [23–25]. The MK test has been widely used for trend detection in hydrological and climatic research since the data does not need to conform to any distribution form, and it allows the

missing data [26,27]. In this research, the missing data were filled due to computation of the ET_0. The change points were detected based on the sequential MK test, which has been largely employed for the detection of change points in different climatic and hydrological data series [28–30]. Detailed information related to the sequential MK test can be found in studies published by Palizdan et al. [29] and Liang et al. [30]. In addition, Sen's slope estimator was used to measure the magnitude of the trend [31]. The MK test and Sen's slope estimator calculations for various time series of climate factors and ET_0 were performed using the Excel-based template MAKESENS 2.0 beta, developed by researchers at the Finnish Meteorological Institute [32].

Linear regression coupled with break trend analysis [33] was applied to calculate the temporal trends of the ET_0 series for the period from 1960–2014. This method is one of the linear trend methods, which divides a certain time series into several periods. The linear regression is used in each period for detecting the temporal trend. A break trend analysis can provide more details about a long term change pattern compared with a simple linear regression. The period for the break trend analysis was chosen as every 30 years, which was considered as the climatological normal period according to the recommendation of the WMO [34]. In this study, the climatological normal ranges were from 1960 to 1989, from 1970 to 1999, from 1980 to 2009, and from 1985 to 2014. It should be noted that in both trend analysis methods, the significance level (α) was set to 0.05 (one-sided t-test).

2.3.3. Sensitivity Analysis

A sensitivity analysis is a quantitative description method for the effect of the input variables on the output [35]. In the present study, it was performed to evaluate the effect of climatic variables on ET_0. Because of the different approaches used in determining ET_0, there are no standard or common procedures for carrying out the sensitivity analyses on ET_0 [20,36]. This study applied the sensitivity analysis method developed from Zhan et al. [37], which has the advantages of simple procedures and evident outcomes of detecting sensitive factors. The measure S_x is the sensitivity of the FAO-PM method to a meteorological parameter, defined as:

$$S_{xij} = \left| \frac{ET_0\langle 1.1xij\rangle - ET_0\langle 0.9xij\rangle}{ET_0\langle xij\rangle} \right| \quad (4)$$

where x_i is a meteorological parameter needed for the calculation of ET_0; j is a given year; $ET_0\langle x_{ij}\rangle$, $ET_0\langle 1.1x_{ij}\rangle$, and $ET_0\langle 0.9x_{ij}\rangle$ are the estimated ET_0 in j year when the parameter x_i equals its value or is 1.1 and 0.9 times its value, respectively. The larger the S_{xij} is, the more sensitivity x_i will have.

2.3.4. Aridity Index (*AI* Index)

Aridity is usually expressed as a comprehensive function of precipitation, temperature, and/or potential evapotranspiration, and reflects the level of meteorological drought [38]. *AI* is defined by Thornthwaite [39], who calculated *AI* as dividing the difference between precipitation and potential evapotranspiration by the potential evapotranspiration. This method is understood as the dearth of water availability at the surface and subsurface levels, can express the aridity degree in arid or semiarid regions, and can help to further analyze drought-wetness variations in terms of agriculture demand [4,40].

In this study, following Thornthwaite [39], the *AI* was computed as:

$$AI = (ET_0 - P)/ET_0 \quad (5)$$

where ET_0 is the reference evapotranspiration, and P is the precipitation. If the *AI* is equal to or close to 1, it indicates that there is no precipitation, and aridity is the highest. In contrast, if the precipitation is equal to or higher than ET_0, the *AI* will be equal to 0 or negative. The *AI* values of the growing season

at each station were calculated, and the average *AI* in the entire Songnen Grassland was expressed by the arithmetic average from the stations in and around the region.

2.3.5. Spatial Interpolation

For analyzing the spatial patterns of ET_0 trends and their magnitudes, the Inverse Distance Weighting algorithm (IDW) was used, which is extensively applied for mapping the spatial extent of climatic and hydrological point data. This method is a simple deterministic interpolation, and assumes that sample values closer to the prediction location are more representative of the prediction value than sample values farther away [41]. Therefore, the closest value to the prediction location gets the greatest weight and the weight is reduced as a function of distance [29]. The power parameter (α), which controls the importance of the predicted location values, is the main factor affecting the result from the IDW method. The α, a positive, real, and constant number, can change from 1 to 5. As a higher α value is selected, more weight is given to the closed location. In this study, α was defined as 2 by following Palizdan et al. [29]. All spatial interpolations were conducted using the ArcGIS 10.2 software.

3. Results

3.1. Spatial Distribution of ET_0, P, and Their Difference over the Period from 1960–2014

The spatial distributions of ET_0 and P annually, seasonally, and during the growing season from 1960 to 2014 are shown in Figure 2, and the difference between the two is displayed using the IDW interpolation as well. Figure 2 shows a strong variability and marked difference between the northeastern ranges and the southwestern region. From the visual inspection, it was observed that the spatial pattern of the high and low values of annual ET_0, P, and their difference all show similarities to the growing season and seasonal time series. The spatial pattern of ET_0 and the difference indicated higher values in the southwest and lower values in the northeast areas, but precipitation showed the opposite trend, in which the minimum value was in the west and the highest value was in the east. Generally, the ET_0 value was more than double the precipitation amounts for all time scales considered, especially for the annual values and during the growing season.

For ET_0, the average of the annual and growing season values increased from the northeast to southwest, with values less than 850 and 750 mm, respectively, to more than 1100 and 980 mm, respectively. Seasonally, all of the stations showed higher ET_0 in the summer, followed by spring, autumn, and winter. For P, the annual value and that of the growing season increased from west to east, ranging from 381 to 577 mm and from 352 to 511 mm, respectively. The minimum was found in Tongyu, and the maximum was found in Changchun. Seasonally, higher amounts of precipitation were exhibited during the summer, followed by autumn, spring, and winter. The maximum difference was distributed in the southwest at all time scales (Figure 2), especially for the annual values, reaching 700–800 mm in the southwest. From a seasonal perspective, the maximum value of the difference occurred in the spring, ranging from 215 to 350 mm and was followed by summer, autumn, and winter.

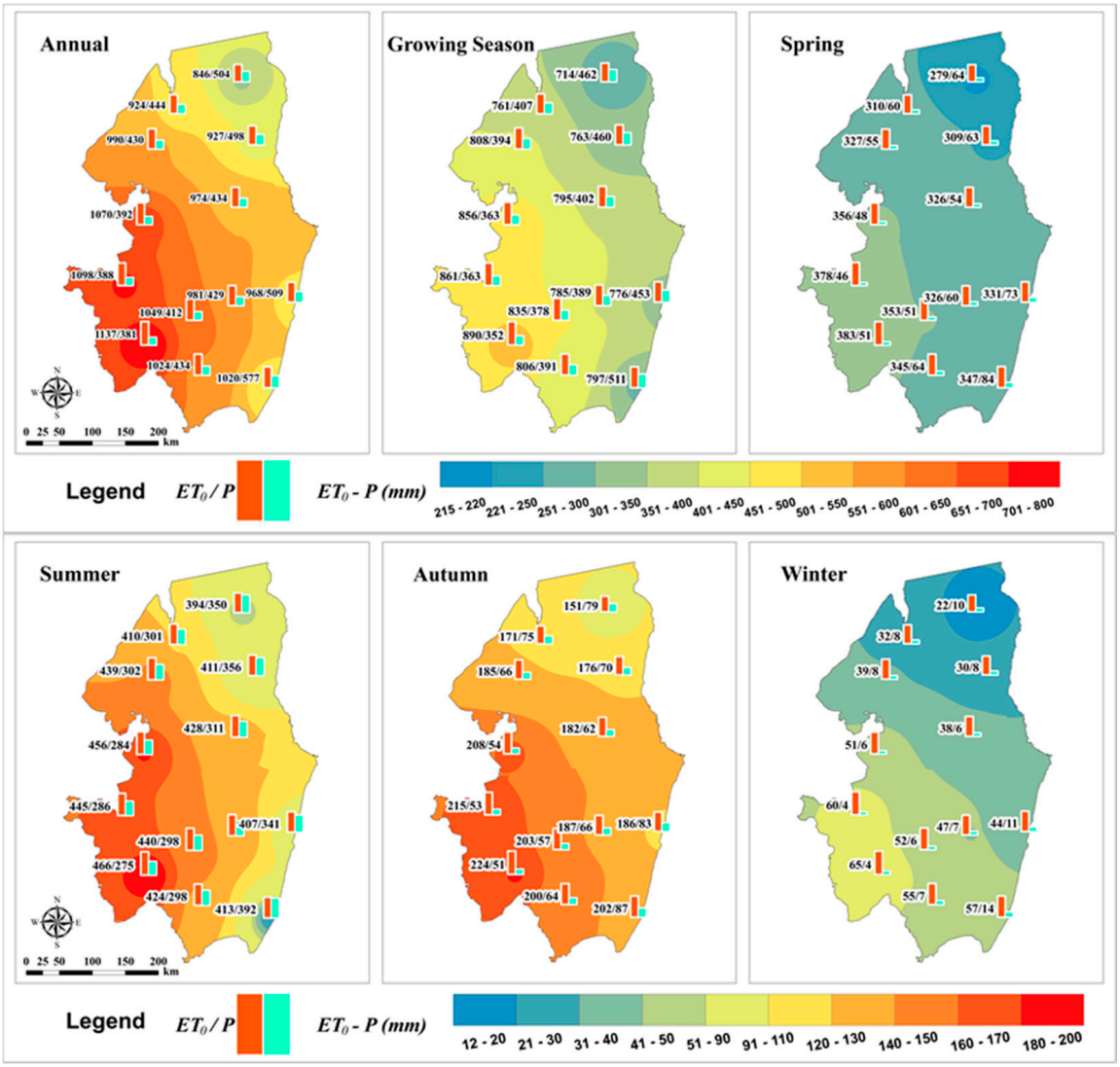

Figure 2. Spatial distribution of ET_0, P, and the difference between the two for the period from 1960–2014.

3.2. Temporal Variations of ET_0

The results of the break trend analysis for the area-averaged annual, seasonal, and the growing season ET_0 time series of the 21 stations during 1960–2014 are shown in Figure 3, and those of the MK test and Sen's slope estimator are summarized in Figure 4. Figure 3 indicates an evident decreasing trend in ET_0 in the annual, seasonal, and growing season time series, especially for the annual, growing season, and spring periods, which passed the significance test at the 0.05 level. In addition, it was shown that almost all annual, seasonal, and the growing season time series had experienced a decreasing trend of ET_0 for the four climatological normal time ranges with the rate ranging from -2.415 to -0.003 mm/a. The sharpest drop rate was detected from 1970 and 1999, and the maximum was in the growing season (-2.415 mm/a). However, it is noteworthy that the region experienced an increasing trend of ET_0 in the annual, seasonal, and the growing season time series during 1980–2009, with a rate ranging from 0.085 to 0.296 mm/a, except in spring and winter, although the increasing trend was not significant. To detect the change points, the MK test was performed in the ET_0 for the annual, seasonal, and the growing season time series during 1960–2014. As shown in Figure 3, both the annual and growing season series have three change points, 1989, 1994, and 2009, and 1989, 1995, and 2008, respectively. Seasonally, in spring, there was a clear change point in 2008; in autumn, four change points were identified, 1972, 1985, 1994, and 2009; in winter, the series had change points at

1977 and 2011. However, there was no detectable change point in summer. The results show that abrupt changes in the ET_0 series mainly occurred in the early and mid-1990s, leading to a fluctuation of ET_0 which is dominated by a decreasing trend.

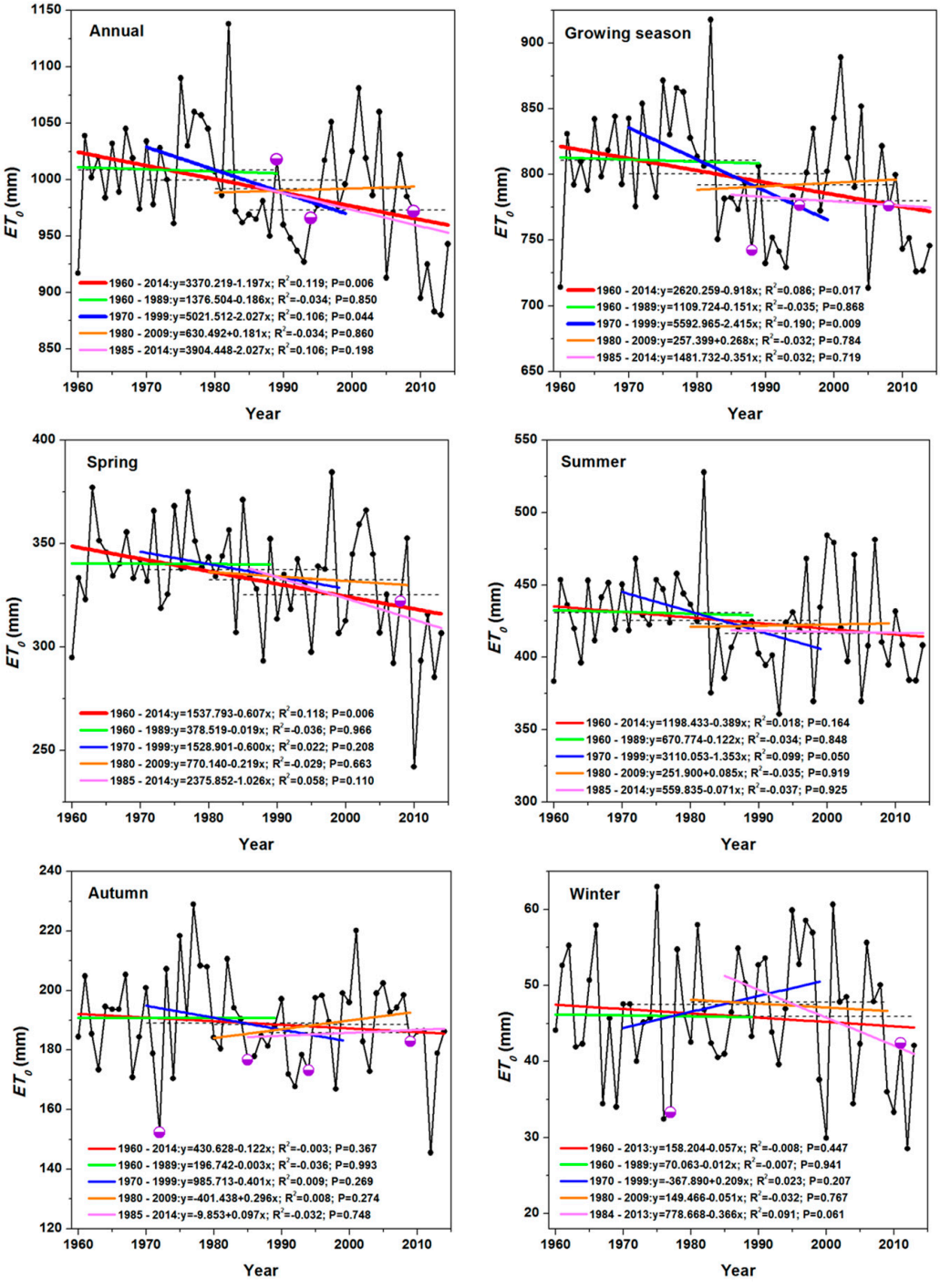

Figure 3. Linear trend and break trend analysis (for every 30 years) of ET_0 from 1960 to 2014. The black dashed line is the average value of the four climatological normal periods. ◒ indicates the detected change point.

The results of the MK test are exhibited in Figure 4, and they are almost identical to those from the linear trend analysis. ET_0 exhibited a decreasing trend in the annual, seasonal, and the growing season time series at the 21 stations during 1960–2014. Overall, more than 90% of the analyzed stations

reported decreasing trends of ET_0 except during autumn and winter, and among those stations about 50% were shown to be decreasing during the annual, growing season, and spring in a statistically significant manner. Increasing trends were found in less than 10% of the data sets, especially during autumn with 38% showing increasing trends, but none of the trends were significant. In terms of the magnitude of the trends, the highest decrease in ET_0 was recorded in Haerbin (around the region) and Fuyu City (inside the region) at the annual level, with an average decrease of -4.45 and -2.86 mm/a, respectively. On the basis of these results, there is no doubt that the Songnen Grassland has experienced an evident decrease in ET_0 over the last 55 years. With decreasing ET_0, the crop or vegetation water demand would be reduced, and the risk of drought would be mitigated. In other words, the decrease in ET_0 rates may mitigate the drought impact on local vegetation and agricultural production.

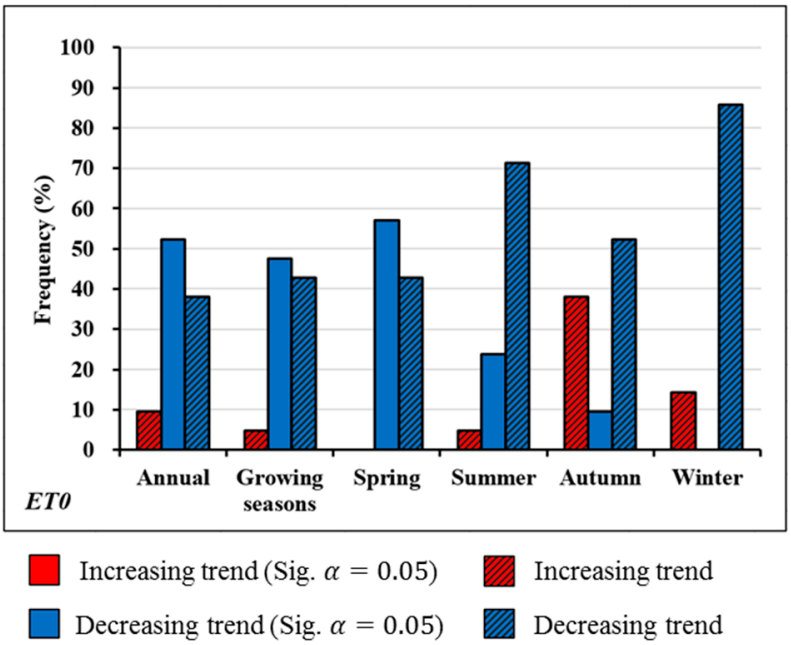

Figure 4. Frequency of ET_0 trends for the 21 stations based on the Mann-Kendall (MK) test in the Songnen Grassland during 1960–2014 (%).

3.3. Spatial Patterns of Trends in ET_0

The spatial variations of ET_0 trends at different time scales from 1960 to 2014 based on the MK test are displayed in Figure 5. All considered time scales indicated a similar pattern, with the majority of the time series of ET_0 indicating a downward trend in the entire region, except during autumn. The greatest number of stations with significant decreasing trends of ET_0 were distributed in the eastern, northeastern, and central regions and frequently occurred in the annual, spring, and growing season periods. These regions also had the highest rate decrease in ET_0, ranging from -0.2 to -4.0 mm/a. However, positive changes were recorded in the southwestern and southern regions in autumn and winter, but they were statistically insignificant, with rate increases ranging from 0.01 to 0.40 mm/a. Overall, the spatial pattern of ET_0 change in the Songnen Grassland is that of a significant downward trend across the central region with a gradually reduced intensity from the eastern parts to the western areas.

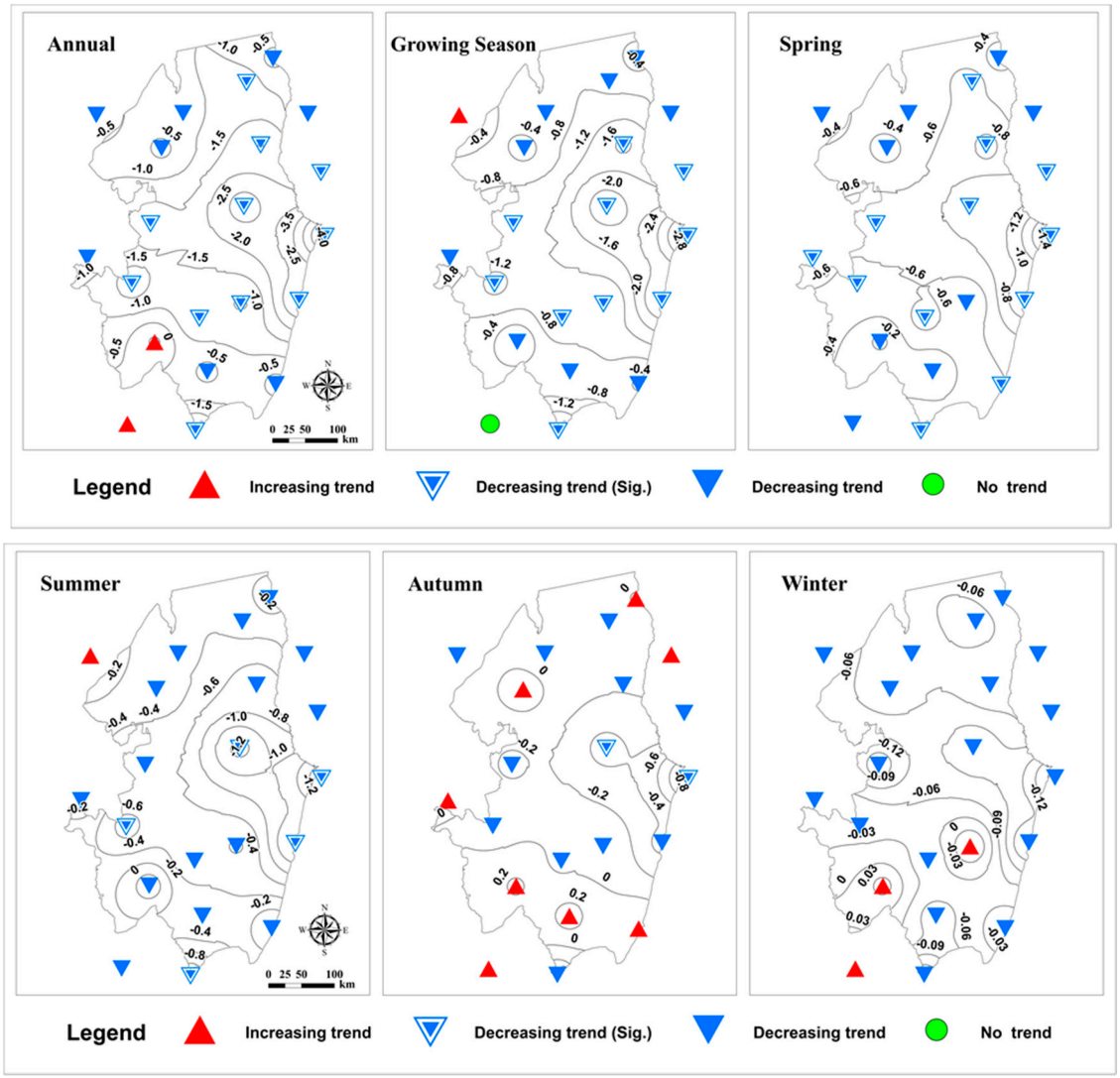

Figure 5. Spatial distribution of trends and their magnitudes in ET_0 over the period from 1960–2014. The Sig. indicates a significant trend at the 0.05 level. The black line is the contour line of the magnitude of the ET_0 trend.

3.4. Changes in the Climatic Parameters

The changes in basic climatic parameters that might play a considerable role in ET_0 change have been investigated for the 21 stations across the Songnen Grassland during 1960–2014. With an increase of air temperature (Ave *T*, Max *T*, and Min *T*), the regional annual Ave *RH*, Sun *H*, and Win *S* all significantly decreased during the study period (Figure 6). All the climatic parameters experienced constant changes during the four climatological normal periods, i.e. from 1960 to 1989, from 1970 to 1999, from 1980 to 2009, and from 1985 to 2014. All the increasing trends of Ave *T*, Max *T*, and Min *T* and the decreasing trends of Sun *H* and Win *S* passed the significance test at the 0.01 level, while the Ave *RH* passed the significance test at the 0.05 level. The MK test was used to detect the change points for each climatic parameter. Each of them has a clear change point around 1990. The change point years of Ave *T*, Max *T*, and Min *T* with significant increasing trends were 1987, 1989, and 1983, respectively. Those of Ave *RH*, Win *S*, and Sun *H* were 1993, 1990, and 1987, respectively. It is worth noting that the time of abrupt changes in Max *T* and Ave *RH* are almost in line with that of the annual ET_0 time series during 1960–2014. In addition, the detected change points for both the annual ET_0 and the climate parameters mainly occurred in the late 1980s and 1990s.

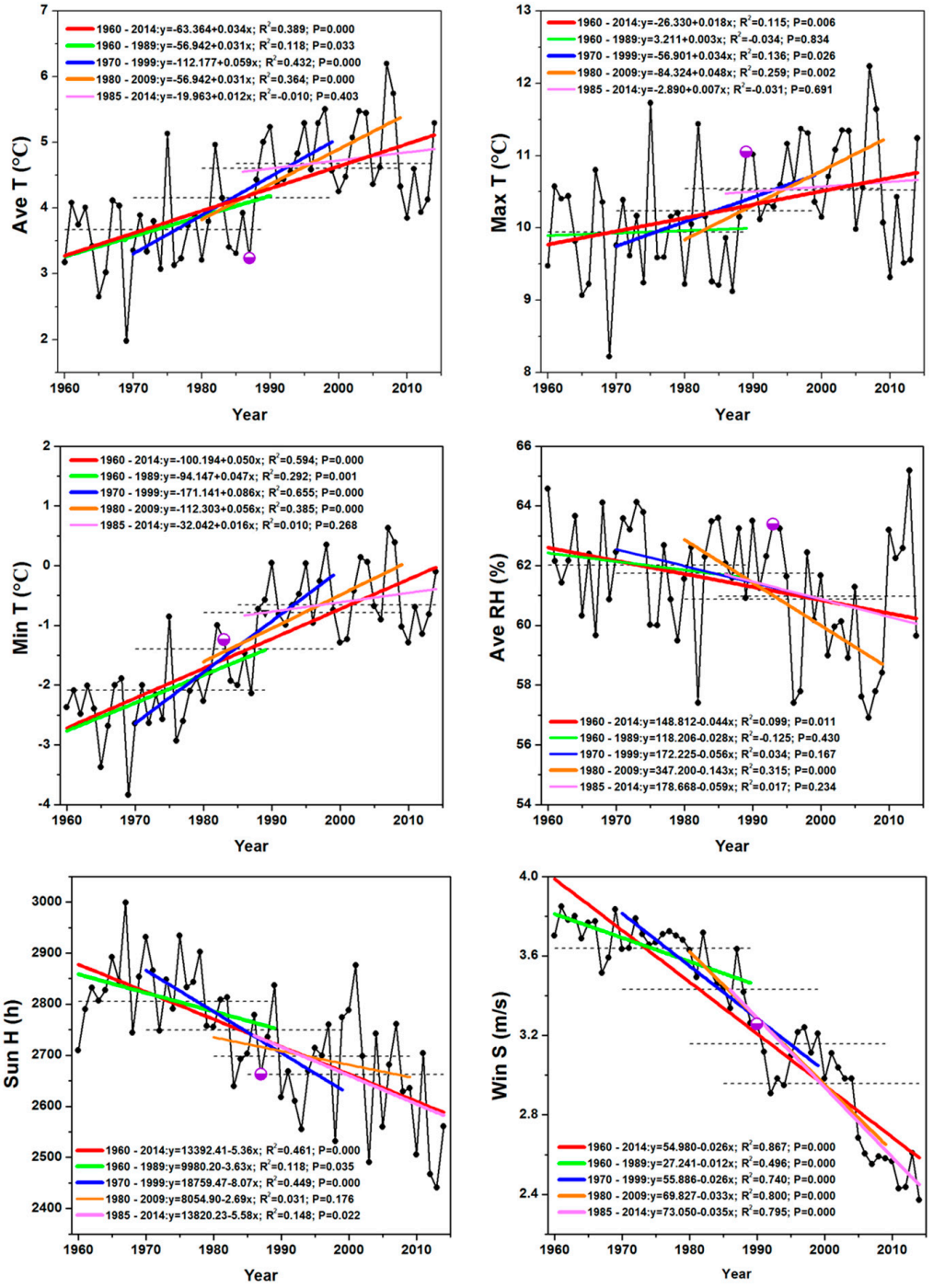

Figure 6. Linear trend and break trend analysis (for every 30 years) of the climatic parameters from 1960 to 2014. ◒ indicates the detected change point.

The MK test was used for detecting the statistical significance of the climatic parameters trends at the 21 stations in the annual, seasonal, and the growing season time series during 1960–2014. The results are summarized in Figure 7. For Ave *T* and Min *T*, the percentage value of the statistically significant increase (α = 0.05) was 100% at all considered time scales, except during winter (95% in Min *T* and more than 70% in Ave *T*). In the case of Sun *H*, all of the annual, seasonal, and growing season series illustrated downward trends, ranging from 52% to 71% and being statistically significant decreases. As for Win *S*, significantly decreasing trends were found roughly 100% of the time at all

locations. For Ave *RH*, an overwhelming majority of data series saw negative trends, but in spring, positive trends were detected at more than 50% of the stations.

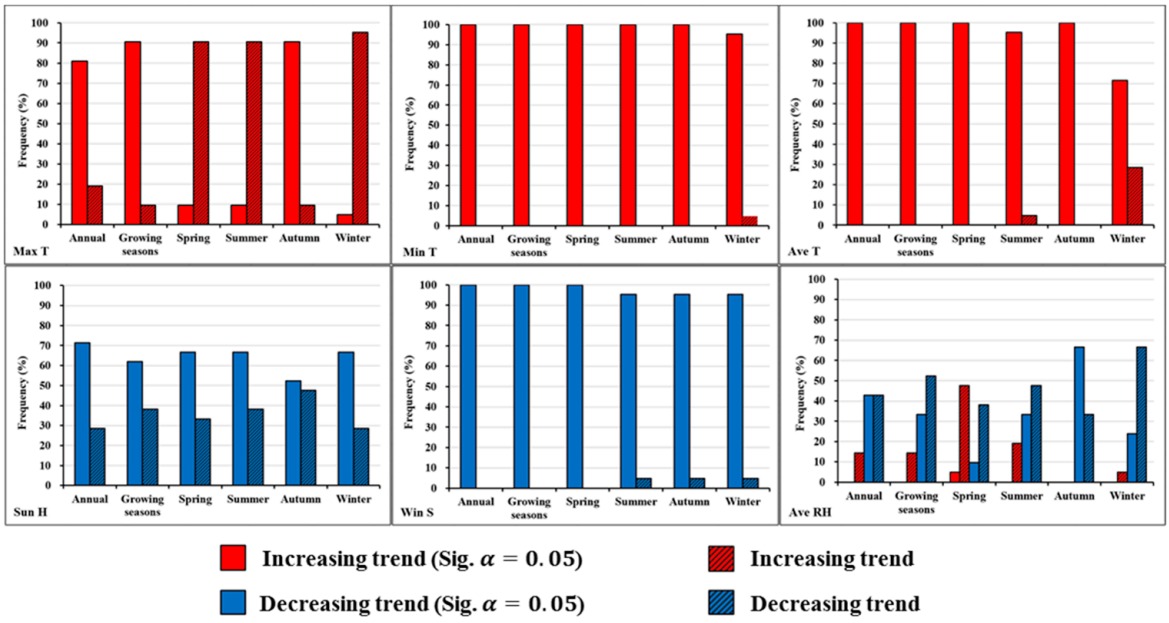

Figure 7. Frequency of climatic parameter trends in the Songnen Grassland over the period from 1960–2014 (%).

3.5. Sensitivity Analysis of Climatic Variables

The results of the sensitivity analysis for annual ET_0 to the climatic variables are given in Figure 8 and Table 1 for the 13 stations inside the Songnen Grassland. It can be seen from Figure 8 that the Ave *RH* and Max *T* were the most sensitive variables to the change in ET_0 over the whole region, and the sensitivity decrease from Win *S*, Sun *H*, Min *T* to Ave *T*. However, there was a small difference in the northeast region at the Keshan and Mingshui stations, which may be the result of the relatively high elevation of the two stations, and there are small hills near those stations. The most sensitive climatic variables at these two stations were Ave *T* and Min *T*, respectively. The summary of the sensitive climatic variables and the temporal trends of their sensitivities based on the MK test are given in Table 1. The results indicate that the sensitivity of Ave *RH* had a significant decreasing trend except at the Anda station, which had a significant increasing trend. The trend of the sensitivity of Max *T* was the same as that of Ave *RH* with a significant downward trend for almost the whole region, except for a significant upward trend in Changchun. For the sensitivity of Win *S* and Min *T*, a majority of stations had a significant increasing trend. Sun *H* had the same temporal trend as Win *S* and Min *T*; but in the southwest region, Tongyu and Changling, there was no significant decreasing trend. As for the sensitivity of Ave *T*, the results showed a slight impact on the changing ET_0 in the Songnen Grassland, except in Keshan. To summarize, the sensitivity of Ave *RH*, Max *T*, Ave *T*, and Min *T* displayed significant decreasing trends, while that of Win *S* and Sun *H* displayed significant increasing trends in the whole region.

Table 1. Summary of the sensitive climatic variables that contributed to the changes in ET_0 at the stations during 1960–2014.

Station	Order and Trend of the Sensitivity for the Climatic Variables in ET_0											
Keshan	*Ave T*	−5.55 *	*Ave RH*	−3.54 *	*Max T*	−3.59 *	*Win S*	−0.81	*Sun H*	3.85 *	*Min T*	0.94
Fuyu	*Ave RH*	−2.38 *	*Max T*	−3.17 *	*Sun H*	2.06 *	*Min T*	1.56	*Win S*	0.07	*Ave T*	1.10
Qiqihaer	*Ave RH*	−4.56 *	*Max T*	−4.15 *	*Win S*	1.31	*Sun H*	2.06 *	*Min T*	4.24 *	*Ave T*	0.00
Mingshui	*Min T*	−6.90 *	*Ave RH*	−3.96 *	*Max T*	−4.85 *	*Win S*	0.64	*Sun H*	1.51	*Ave T*	0.00
Tailai	*Ave RH*	−3.89 *	*Max T*	−3.12 *	*Win S*	4.02 *	*Sun H*	1.29	*Min T*	3.66 *	*Ave T*	0.00
Anda	*Ave RH*	2.83 *	*Max T*	−3.56 *	*Win S*	0.20	*Sun H*	4.07 *	*Min T*	0.40	*Ave T*	0.00
Baicheng	*Ave RH*	−3.05 *	*Max T*	−3.03 *	*Win S*	1.19	*Sun H*	1.80	*Min T*	2.08 *	*Ave T*	0.00
Qian'an	*Ave RH*	−2.90 *	*Max T*	−2.87 *	*Win S*	2.53 *	*Sun H*	0.28	*Min T*	1.68	*Ave T*	0.00
Qian Gorlos	*Ave RH*	−6.27 *	*Max T*	−4.66 *	*Win S*	0.96	*Sun H*	3.53 *	*Ave T*	−4.72 *	*Min T*	2.31 *
Tongyu	*Ave RH*	−2.95 *	*Max T*	−1.74	*Win S*	3.03 *	*Sun H*	−0.15	*Min T*	1.06	*Ave T*	0.00
Changling	*Ave RH*	−3.27 *	*Max T*	−2.63 *	*Win S*	4.01 *	*Sun H*	−1.26	*Min T*	2.42 *	*Ave T*	0.00
Fuyu City	*Ave RH*	−5.62 *	*Max T*	−4.37 *	*Win S*	2.42 *	*Sun H*	1.28	*Min T*	3.14 *	*Ave T*	0.00
Changchun	*Max T*	3.11 *	*Ave RH*	−6.11 *	*Win S*	1.97 *	*Sun H*	3.47 *	*Min T*	2.24 *	*Ave T*	0.00
Region	*Ave RH*	−4.07 *	*Max T*	−4.18 *	*Win S*	2.90 *	*Sun H*	3.92 *	*Ave T*	−6.94 *	*Min T*	−7.93 *

Notes: The order means the ranking of the sensitive climatic variables (descending) at each station. The trends of the sensitivity for the climatic variables were detected by the MK test. * Indicates a significance level of 0.05.

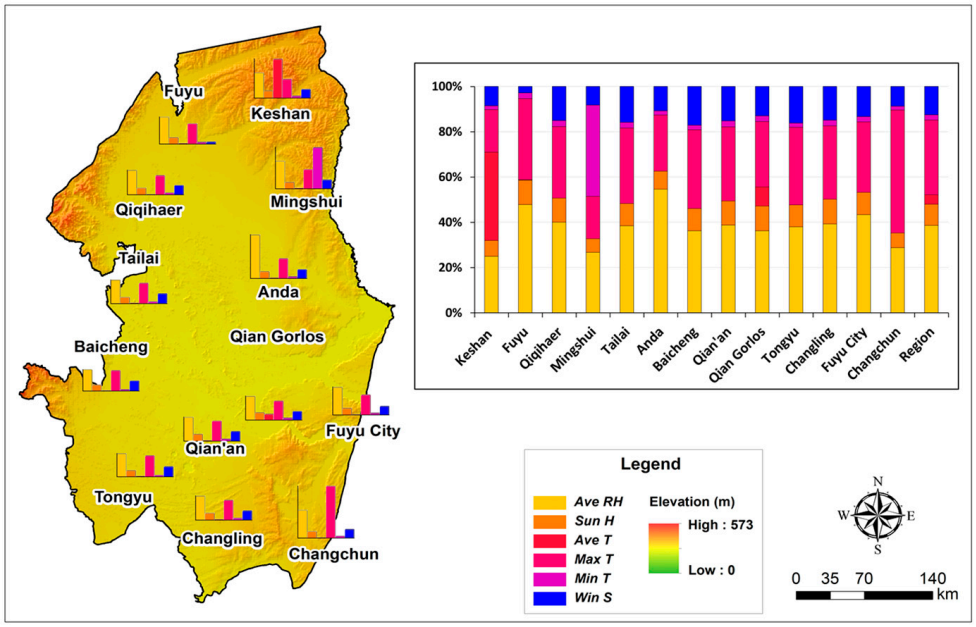

Figure 8. Spatial distribution of the average annual sensitivities of the climatic variables and the result of the sensitivity comparison in 13 inside stations during 1960–2014.

3.6. The Role of ET_0 in Regional Dry/Wet Conditions

The ratio of ET_0 during the growing season to the total annual amount was computed from 1960 to 2014. Results show that, in general, the total ET_0 in growing season accounts for more than 80% within the year. As this period is critical for crop and vegetation growth, it directly affects regional socioeconomic development. Therefore, this study only considers the role that ET_0 may play in regional dry/wet conditions during the growing season. Regional trends and the magnitudes of ET_0, AI, and P were analyzed at two spatial scales, at the 13 inside stations and at the 21 stations which takes the adjacent stations into account, respectively. However, only the results of the 13 interior stations are presented in Figure 8, due to the similarity of the results for the analysis of the trends and the magnitudes of ET_0, AI, and P at the 21 stations.

Figure 9 gives the interannual variations of the growing season ET_0, AI, and P over the Songnen Grassland for the period from 1960 to 2014. From the visual inspection, ET_0, AI, and P all displayed decreasing trends, but only the decreasing trend of ET_0 passed the significance test. As for the fluctuation in temporal evolution, the results indicated that the fluctuating pattern of ET_0 was similar

to AI, but opposite that of P. A simple regression equation was established between ET_0, AI, and P based on the SPSS Statistics 19.0 Software. The equation is as follows:

$$AI = 63.81 - 0.125P + 0.046ET_0 \left(R^2 = 0.98,\ P = 0.00\right) \quad (6)$$

Equation (6) indicates a positive correlation between AI and ET_0 and a negative correlation between AI and P. The regression residual standard error is displayed in Figure 10 to test the validity and accuracy of Equation (6). It indicated that the residuals are approximately normally distributed since all 55 residuals are distributed around the diagonal line, and it also illustrated that the regression equation (Equation (6)) is in line with the normal distribution. Thus, Equation (6) is statistically significant. Furthermore, the upward trends of ET_0 and AI were associated with the downward trends of P and vice versa. This characteristic was highly explicit during the drought and wet years in particular. As shown in Figure 10, during the severe drought years D1 (1982), D2 (2001), D3 (2004), and D4 (2007), the values of ET_0 and AI had reached or were close to the maximum in the last few decades; however, the values of P had almost reached a minimum at the same time. Similarly, the wet years, such as W1 (1960), W2 (1998), and W3 (2013) had lower values of ET_0 and AI (Figure 9).

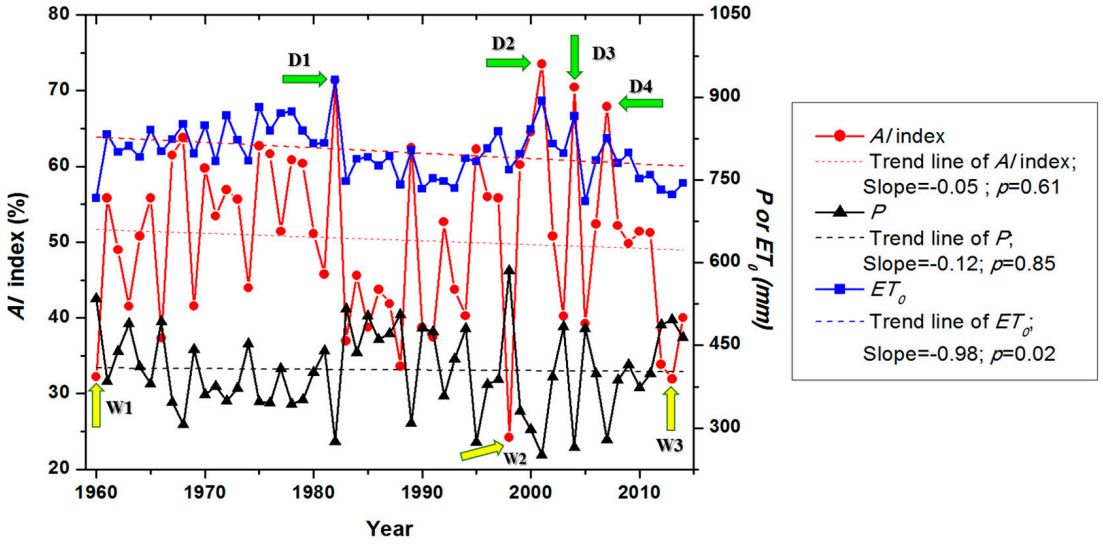

Figure 9. Comparison of the temporal trend of ET_0, AI, and P during 1960–2014. D, the drought year; W, the wet year. The slopes are examined by linear regression.

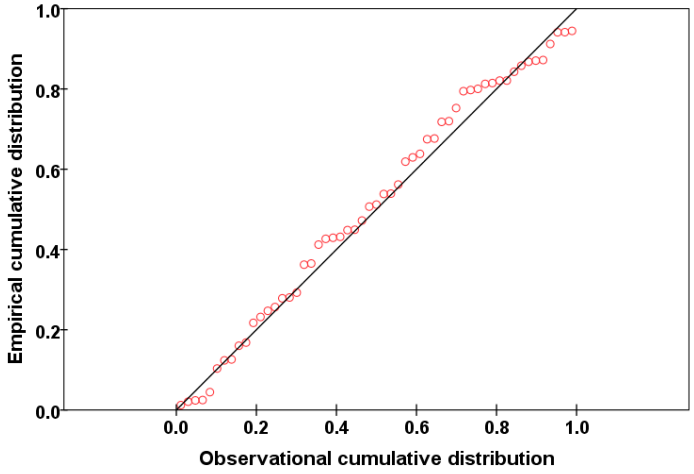

Figure 10. P-P plot of the regression residual standard error for ET_0, AI, and P.

4. Discussion

The Songnen Grassland shows obvious spatial variations of ET_0 rates from the northeast to southwest at different time scales (Figure 2). These variations are influenced by different regional climates and local topography. In the northeast and east, the temperature is comparatively low, because there were some valleys and the stations were located in a relatively high latitude area combined with the cold temperate continental monsoon climate, leading to the lower values of ET_0 in these areas; while in the southwest, the topography was relatively flat at lower latitudes (Figure 1), in addition to being far away from the ocean, resulting in the lower relative humidity and the higher values of ET_0. Moreover, in this study, the IDW method could affect the accuracy of the spatial distribution as well. Previous studies indicated that the interpolation methods should account for external factors, such as altitude and land use patterns [42]. However, compared with other interpolation methods, the IDW produced slightly better predictions of ET_0 [29,43]. Future studies should consider how different interpolation methods impact the spatial variations of ET_0 at different time scales.

Moreover, the trend analyses of ET_0 at different time scales by linear regression and non-parametric tests were consistent. Results show that the ET_0 rates over the Songnen Grassland have been decreasing over the last few decades (Figures 3–5). The results were consistent with decreasing trends in the lower reaches of the Taoer River basin in Northeast China investigated by Liang et al. [30]. Huo et al. [4] also reported a decreasing trend in the arid area of northwest China during 1955–2008. However, as discussed in the introduction, some studies have identified increasing trends in some regions during the last few decades. One of the reasons for the inconsistent findings in ET_0 trends is due to the fact that some studies on climate change utilize divergent climatic parameters, potentially providing incomplete or artificial trends and magnitudes of ET_0 [11].

During the study period, the observed variations in Max T, Min T, and Ave T were similar to the global pattern of increasing minimum, mean, and maximum temperature [12]; and the results of the analysis of other climatic factors were consistent with the findings reported from Yunnan Province in southwest China during 1961–2004 [5]. There, the sensitivity analyses for changes in the annual ET_0 showed that Ave RH and Max T were the most sensitive climate variables over the whole Songnen Grassland, which was in agreement with Yin et al. [44], who studied all of China during 1961–2008. However, Liu et al. [14] has reported that Win S and Sun H were the most sensitive factors in other parts of China. Therefore, it can be concluded that ET_0 has different responses to climate variables in different regions and under different climate conditions. The reasons for the inconsistent responses of ET_0 may be the geographical position (e.g., distance from the ocean, the altitude variations) and the research period. In addition, this study indicates that the increase of ET_0 induced by rising air temperature can be compensated by the reduced ET_0 with the significant decrease of Ave RH, Win S, and Sun H. As a result, the regional ET_0 appeared to show a declining trend. Human activity could account for some of the local climate change [36], such as greenhouse gas (GHG) emissions and rapid urbanization, which should be further studied in the Songnen Grassland. In addition, the existence of natural climate variability may also affect the ET_0 trends. Further research should focus on how to identify the effect of climate natural variability in the changes of ET_0, for better understanding of the mechanism of ET_0 variations.

Comparing the results of the detected change points of ET_0 with the climatic factors in the annual time scale during 1960–2014, abrupt changes were detected in 1989, 1994, and 2009, while the most sensitive factors, Ave RH and Max T, were detected in 1993 and 1989. There is a good correspondence between these two sensitive factors and the ET_0 series. However, undoubtedly, the abrupt change of other climate factors also played an important role in the abrupt changes of ET_0. From 1989 to 1994, the ET_0 experienced an abrupt decreasing trend due to the abrupt increasing trend of Max T, Min T, and Ave T, and decreasing trend of Sun H and Win S; the Ave RH also experienced an increasing trend until it reached the year of abrupt change in 1993. From 1994 to 2009, the ET_0 experienced an abrupt increasing trend arising from the abrupt increasing trend of Max T, Min T, and Ave T, and the decreasing trend of Ave RH, Sun H, and Win S. After 2009, the temporal trend of ET_0 decreased

again, although no change points of the climate factors were detected. This can be due to, as shown in Figure 3, the decreasing trends of every climate parameter except for the Ave *RH*.

As a whole, the abrupt changes of ET_0 and its related climatic factors mainly occurred in the early and mid-1990s, and it may be concluded that climate variations were more dramatic since this period, when the air temperature remarkably increased, with decreasing trends of Ave *RH*, Win *S*, and Sun *H*. This period of abrupt surface warming was consistent with Dong et al. [45], who reported an abrupt increase in summer mean surface air temperature over Northeast Asia since the mid-1990s. Accompanying the above mentioned climatic anomalies, a decrease in ET_0 in the Songnen Grassland was observed. In addition, previous studies indicated that the northeast China climate is affected by both the thermal contrast between the Asian continent and the tropical Indo-Pacific Oceans and that between the continent and the extratropical North Pacific [46]. The western Pacific subtropical high (significant positive correlation with summer temperature at the 0.05 level during 1994–2012), zonal circulation (same as above), and Arctic Oscillation (high positive correlation with winter temperature during 1951–1999) also have strong correlations with regional climate variations over northeast China [47,48]. The temperature is one of the most sensitive factors for the change in ET_0, therefore, the large-scale atmospheric and ocean circulation may be other reasons for the abrupt change and variations in ET_0. Future studies should be focused on these effects on the changes in ET_0 in the Songnen Grassland.

ET_0 variations and its response to regional dry/wet conditions are of great importance for crop growing and natural vegetation [3,49]. For this purpose, the present study analyzed the long term variations of ET_0, *AI*, and *P* for the growing season during 1960–2014. The results showed that ET_0 and *AI* decreased as the *P* increased, especially during drought or wet years and vice versa (Figure 10). This was consistent with Madhu et al. [33], who reported that higher *ET* values were detected in the moderate and severe droughts years. It could be inferred from Equation (6) that *AI* has a positive correlation with ET_0 and a negative correlation with *P*. The correlation was analyzed by the Pearson correlation analysis, and the results showed that *AI* has a significant positive correlation with ET_0 ($r = 0.766$, $p = 0.00$), and it has a significant negative correlation with *P* ($r = -0.977$, $p = 0.00$). Figure 9 shows that all the trends of ET_0, *AI*, and *P* were decreasing during the growing season from 1960–2014, and the decreasing rate of ET_0 was higher than that of *P*. Thus, with the significant decreasing trend of ET_0, the climate in the Songnen Grassland became slightly wetter from 1960–2014, and the trend will be continued if the decreasing trend of ET_0 and no obvious change of precipitation persists. In short, under the decreasing ET_0 conditions, agricultural and ecological water requirements will decrease, especially during the growing season, and agriculture irrigation water requirements will reduce as well. These could have a positive influence for vegetation growth, agricultural production, and ecology.

5. Conclusions

In this study, the spatial distributions of ET_0, *P*, and their difference were obtained at different time scales. The temporal and spatial variations of ET_0 were determined for 55 years of data from 21 stations in and around the Songnen Grassland, northeast China, during 1960–2014. The interannual variability of climatic variables was investigated during the study period, and a sensitivity analysis was conducted. The role of ET_0 in regional dry/wet conditions was discussed based on the analysis of the relationship between ET_0, *P*, and *AI*. The following conclusions can be drawn from this study.

(1) The trend analysis of ET_0 at different time scales shows an evident decreasing trend over the last 55 years, especially in the annual and spring periods. A break trend analysis shows that almost all considered climatological normal periods had experienced the decreasing trend, with a range of −2.415 to −0.003 mm per year. Abrupt changes were mainly detected in the early and mid-1990s in the annual, seasonal, and the growing season time series of ET_0.

(2) The spatial distributions of ET_0 increased from the northeast to southwest in the annual, seasonal, and the growing season time series during 1960–2014. The spatial variations of ET_0 indicated that

the most significant decreasing trends were distributed in the eastern, northeastern, and central regions during the annual, spring, and growing season periods.

(3) The interannual variability of climatic parameters indicated that the annual Max T, Ave T, and Min T displayed significant increasing trends at the 0.05 level (one-sided t-test), and significant decreasing trends were found for Ave RH, Win S, and Sun H. Ave RH was the dominant climate variable for the declining annual ET_0 over the entire region, with the sensitivity decreasing from Max T, Win S, Sun H, Min T, to Ave T. Abrupt changes were detected in the annual time series of these variable; Ave RH in 1993, Max T in 1989, Win S in 1990, Sun H in 1987, Min T in 1983, and Ave T in 1987.

(4) In general, the results of this study indicate that the regional drought/wetness condition became mildly wetter with decreasing ET_0 during the growing season in the last 55 years. Regional climate drought has been alleviated in recent decades. These findings can serve as a reference for policy-makers for better planning and efficient use of agricultural water resources in the Songnen Grassland.

Acknowledgments: This study was financially supported by the National Key Technology R&D Program of China under Grant Nos. 2013BAK05B02 and 2013BAK05B01. The authors are grateful to the anonymous reviewers for their insightful and constructive comments for improving this manuscript.

Author Contributions: Jiquan Zhang was responsible for the original idea of the study; Caiyun Sun and Enliang Guo were responsible for the data compilation; Feng Zhang and Mengmeng Wang were responsible for the data processing and drawing; Qiyun Ma drafted the manuscript and all authors read and revised the final manuscript.

Conflicts of Interest: The authors declare no conflict of interest.

References

1. Stephens, G.L.; Hu, Y.X. Are climate-related changes to the character of global-mean precipitation predictable? *Environ. Res. Lett.* **2010**, *5*, 025209. [CrossRef]
2. Escribano Frances, G.; Quevauviller, P.; San Martin Gonzalez, E.; Vargas Amelin, E. Climate change policy and water resources in the EU and Spain. A closer look into the Water Framework Directive. *Environ. Sci. Policy* **2017**, *69*, 1–12. [CrossRef]
3. Croitoru, A.; Piticar, A.; Dragotă, C.S.; Burada, D.C. Recent changes in reference evapotranspiration in Romania. *Glob. Planet. Chang.* **2013**, *111*, 127–136. [CrossRef]
4. Huo, Z.; Dai, X.; Feng, S.; Kang, S.; Huang, G. Effect of climate change on reference evapotranspiration and aridity index in arid region of China. *J. Hydrol.* **2013**, *492*, 24–34. [CrossRef]
5. Fan, Z.; Thomas, A. Spatiotemporal variability of reference evapotranspiration and its contributing climatic factors in Yunnan Province, SW China, 1961–2004. *Clim. Chang.* **2013**, *116*, 309–325. [CrossRef]
6. Lu, J.; Zhang, G.; Wu, F. Web-based Multi-Criteria Group Decision Support System with Linguistic Term Processing Function. *IEEE Intell. Inform. Bull.* **2005**, *5*, 35–43.
7. Naderpour, M.; Lu, J.; Zhang, G. An intelligent situation awareness support system for safety-critical environments. *Decis. Support Syst.* **2014**, *59*, 325–340. [CrossRef]
8. Shadmani, M.; Marofi, S.; Roknian, M. Trend Analysis in Reference Evapotranspiration Using Mann-Kendall and Spearman's Rho Tests in Arid Regions of Iran. *Water Resour. Manag.* **2012**, *26*, 211–224. [CrossRef]
9. Tabari, H.; Aghajanloo, M.B. Temporal pattern of aridity index in Iran with considering precipitation and evapotranspiration trends. *Int. J. Clim.* **2013**, *33*, 396–409. [CrossRef]
10. Wang, Y.; Jiang, T.; Bothe, O.; Fraedrich, K. Changes of pan evaporation and reference evapotranspiration in the Yangtze River basin. *Theor. Appl. Climatol.* **2007**, *90*, 13–23. [CrossRef]
11. Irmak, S.; Kabenge, I.; Skaggs, K.E.; Mutiibwa, D. Trend and magnitude of changes in climate variables and reference evapotranspiration over 116-yr period in the Platte River Basin, central Nebraska–USA. *J. Hydrol.* **2012**, *420–421*, 228–244. [CrossRef]
12. Roderick, M.L.; Farquhar, G.D. Changes in New Zealand pan evaporation since the 1970s. *Int. J. Climatol.* **2005**, *25*, 2031–2039. [CrossRef]
13. Bandyopadhyay, A.; Bhadra, A.; Raghuwanshi, N.S.; Singh, R. Temporal trends in estimates of reference evapotranspiration over India. *J. Hydrol. Eng.* **2009**, *14*, 508–515. [CrossRef]

14. Liu, T.; Li, L.; Lai, J.; Liu, C.; Zhuang, W. Reference evapotranspiration change and its sensitivity to climate variables in southwest China. *Theor. Appl. Climatol.* **2016**, *125*, 1–10. [CrossRef]
15. Dinpashoh, Y.; Jhajharia, D.; Fakheri-Fard, A.; Singh, V.P.; Kahya, E. Trends in reference crop evapotranspiration over Iran. *J. Hydrol.* **2011**, *375*, 65–77. [CrossRef]
16. Liu, Y.; Zhuang, Q.; Pan, Z.; Miralles, D.; Tchebakova, N.; Kicklighter, D.; Chen, J.; Sirin, A.; He, Y.; Zhou, G.; et al. Response of evapotranspiration and water availability to the changing climate in Northern Eurasia. *Clim. Chang.* **2014**, *126*, 413–427. [CrossRef]
17. Zheng, S.; Qin, Z.; Zhang, W. Drought variation in Songnen Plain and its response to climate change. *Chin. J. Agrometeorol.* **2015**, *36*, 640–649.
18. Zhang, Y.; Deng, J.; Guan, D.; Jin, C.; Wang, A.; Wu, J.; Yuan, F. Spatiotemporal changes of potential evapotranspiration in Songnen Plain of Northeast China. *Chin. J. Appl. Ecol.* **2011**, *22*, 1702–1710.
19. Limin, S.G.; Oue, H.; Takase, K. Estimation of areal average rainfall in the mountainous Kamo River Watershed, Japan. *J. Agric. Meteorol.* **2015**, *71*, 90–97. [CrossRef]
20. Allen, R.G.; Pereira, L.S.; Raes, D.; Smith, M. *Crop Evapotranspiration-Guidelines for Computing Crop Water Requirements—FAO Irrigation and Drainage*; FAO: Rome, Italy, 1998; p. 56.
21. Mosaedi, A.; Sough, M.G.; Sadeghi, S.; Mooshakhian, Y.; Bannayan, M. Sensitivity analysis of monthly reference crop evapotranspiration trends in Iran: A qualitative approach. *Theor. Appl. Climatol.* **2017**, *128*, 857–873. [CrossRef]
22. Liu, C.; Zhang, D.; Liu, X.; Zhao, C. Spatial and temporal change in the potential evapotranspiration sensitivity to meteorological factors in China (1960–2007). *J. Geogr. Sci.* **2012**, *22*, 3–14. [CrossRef]
23. Kendall, M.G. *Rank Correlation Methods*; Griffin: London, UK, 1948.
24. Mann, H.B. Nonparametric tests against trend. *Econometrica* **1945**, *13*, 245–259. [CrossRef]
25. Wang, W.; Zhu, Y.; Xu, R.; Liu, J. Drought severity change in China during 1961–2012 indicated by SPI and SPEI. *Nat. Hazards* **2015**, *75*, 2437–2451. [CrossRef]
26. Zhang, Q.; Zhang, J. Drought hazard assessment in typical corn cultivated areas of China at present and potential climate change. *Nat. Hazards* **2016**, *81*, 1323–1331. [CrossRef]
27. Yan, T.; Shen, Z.; Bai, J. Spatial and temporal changes in temperature, precipitation, and streamflow in the Miyun Reservoir Basin of China. *Water* **2017**, *9*, 78. [CrossRef]
28. Tabari, H.; Taye, M.T.; Willems, P. Statistical assessment of precipitation trends in the upper Blue Nile River basin. *Stoch. Environ. Res. Risk Assess.* **2015**, *29*, 1751–1961. [CrossRef]
29. Palizdan, N.; Falamarzi, Y.; Huang, Y.F.; Lee, T.S. Precipitation trend analysis using discrete wavelet transform at the Langat River Basin, Selangor, Malaysia. *Stoch. Environ. Res. Risk Assess.* **2017**, *31*, 853–877. [CrossRef]
30. Liang, L.; Li, L.; Liu, Q. Temporal variation of reference evapotranspiration during 1961–2005 in the Taoer River basin of Northeast China. *Agric. For. Meteorol.* **2010**, *150*, 298–306. [CrossRef]
31. Sen, P.K. Estimates of the regression coefficient based on Kendall's tau. *J. Am. Stat. Assoc.* **1968**, *63*, 1379–1389. [CrossRef]
32. Salmi, T.; Maatta, A.; Anttila, P.; Ruoho-Airola, T.; Amnell, T. *Detecting Trends of Annual Values of Atmospheric Pollutants by the Mann-Kendall Test and Sen's Slope Estimates—The Excel Template Application MAKESENS*; Publications on Air Quality 31; Report Code FMIAQ-31; Universitas Gadjah Mada: Yogyakarta, The Republic of Indonesia, 2002.
33. Madhu, S.; Kumar, T.V.L.; Barbosa, H.; Rao, K.K.; Bhaskar, V.V. Trend analysis of evapotranspiration and its response to droughts over India. *Theor. Appl. Climatol.* **2015**, *121*, 41–51. [CrossRef]
34. Arguez, A.; Vose, R.S. The Definition of the Standard WMO Climate Normal: The Key to Deriving Alternative Climate Normals. *Bull. Am. Meteorol. Soc.* **2011**, *92*, 699–704. [CrossRef]
35. Zhao, L.; Xia, J.; Sobkowiak, L.; Li, Z. Climatic characteristics of reference evapotranspiration in the Hai River Basin and their attribution. *Water* **2014**, *6*, 1482–1499. [CrossRef]
36. Zheng, C.; Wang, Q. Spatiotemporal pattern of the global sensitivity of the reference evapotranspiration to climatic variables in recent five decades over China. *Stoch. Environ. Res. Risk. Assess.* **2015**, *29*, 1937–1947. [CrossRef]
37. Zhan, X.; Kustas, W.P.; Humes, K.S. An intercomparison study on models of sensible heat flux over partial canopy surfaces with remotely sensed surface temperature. *Remote Sens. Environ.* **1996**, *58*, 242–256. [CrossRef]
38. Su, X.; Singh, V.P.; Niu, J.; Hao, L. Spatiotemporal trends of aridity index in Shiyang River basin of northwest China. *Stoch. Environ. Res. Risk. Assess.* **2015**, *29*, 1571–1582. [CrossRef]

39. Thornthwaite, C.W. An approach toward a rational classification of climate. *Geogr. Rev.* **1948**, *38*, 55–89. [CrossRef]
40. Zhang, K.; Pan, S.; Zhang, W.; Xu, Y.; Cao, L.; Hao, Y.; Wang, Y. Influence of climate change on reference evapotranspiration and aridity index and their temporal-spatial variations in the Yellow River Basin, China, from 1961 to 2012. *Quat. Int.* **2015**, *380–381*, 75–82. [CrossRef]
41. Ashraf, M.; Routray, J.K. Spatio-temporal characteristics of precipitation and drought in Balochistan Province, Pakistan. *Nat. Hazards* **2015**, *77*, 229–254. [CrossRef]
42. Li, X.; Gemmer, M.; Zhai, J.; Liu, X.; Su, B.; Wang, Y. Spatio-temporal variation of actual evapotranspiration in the Haihe River Basin of the past 50 years. *Quat. Int.* **2013**, *304*, 133–141. [CrossRef]
43. Piticar, A.; Mihăilă, D.; Lazurca, L.G.; Bistricean, P.; Puţuntică, A.; Briciu, A. Spatiotemporal distribution of reference evapotranspiration in the Republic of Moldova. *Theor. Appl. Climatol.* **2016**, *124*, 1133–1144. [CrossRef]
44. Yin, Y.; Wu, S.; Chen, G.; Dai, E. Attribution analyses of potential evapotranspiration changes in China since the 1960s. *Theor. Appl. Climatol.* **2010**, *101*, 19–28. [CrossRef]
45. Dong, B.; Sutton, R.T.; Chen, W.; Liu, X.; Lu, R.; Sun, Y. Abrupt summer warming and changes in temperature extremes over Northeast Asia since the mid-1990s: Drivers and physical processes. *Adv. Atmos. Sci.* **2016**, *33*, 1005–1023. [CrossRef]
46. Liu, S.; Yang, S.; Lian, Y.; Zheng, D.; Wen, M.; Tu, G.; Shen, B.; Gao, Z.; Wang, D. Time–frequency characteristics of regional climate over northeast China and their relationships with atmospheric circulation patterns. *J. Clim.* **2010**, *23*, 4956–4972. [CrossRef]
47. Gong, D.Y.; Wang, S.W. Influence of Arctic Oscillation on Winter Climate over China. *J. Geogr. Sci.* **2003**, *13*, 208–216.
48. Li, J.; Jiao, M.; Hu, C.; Li, F.; Zhang, X.; Zhang, Q.; Wang, Y.; Zhu, X. Characteristics of summer temperature and its impact factors in Northeast China from 1951 to 2012. *J. Meteorol. Environ.* **2016**, *32*, 74–83.
49. Espadafor, M.; Lorite, I.J.; Gavilan, P.; Berengena, J. An analysis of the tendency of reference evapotranspiration estimates and other climate variables during the last 45 years in Southern Spain. *Agric. Water Manag.* **2011**, *98*, 1045–1061. [CrossRef]

© 2017 by the authors. Licensee MDPI, Basel, Switzerland. This article is an open access article distributed under the terms and conditions of the Creative Commons Attribution (CC BY) license (http://creativecommons.org/licenses/by/4.0/).